Optical Droplet Vaporization of Micron-sized Perfluorocarbon Droplets and their Photoacoustic Detection

Eric Strohm[a], Min Rui[a], Ivan Gorelikov[b], Naomi Matsuura[b], Michael Kolios[a]
[a]Department of Physics, Ryerson University, Toronto, Canada;
[b]Imaging Research Department, Sunnybrook Health Sciences Centre, Toronto, Canada
mkolios@ryerson.ca

ABSTRACT

An acoustic and photoacoustic characterization of micron-sized perfluorocarbon (PFC) droplets is presented. PFC droplets are currently being investigated as acoustic and photoacoustic contrast agents, as well as cancer therapy agents. Pulse echo measurements at 375 MHz were used to determine the PFC diameter of nine droplets, ranging from 3.2 to 6.7 μm, and the PFC sound velocity, ranging from 311 to 406 m/s. An average sound velocity of 379 ± 18 m/s was calculated if droplets smaller than the ultrasonic beam width of 4.0 μm were excluded. Optical droplet vaporization, where vaporization of a single droplet occurred upon laser irradiation of sufficient intensity (above 1.5 J/cm^2), was verified using acoustic methods. The ultrasonic backscatter amplitude, acoustic impedance and attenuation increased after vaporization, consistent with a phase change from a liquid to gas core. Using laser irradiation values below the vaporization threshold, photoacoustic measurements were used to compare the photoacoustic ultrasound emission spectra of three droplets of varying diameters to a theoretical model. Good agreement of the experimental results with theoretical predictions of the ultrasound spectral features were observed over the bandwidth of the 375 MHz transducer.

Keywords: Perfluorocarbon droplets, contrast agent, nanoparticles, acoustic microscopy, photoacoustic imaging

1. INTRODUCTION

Liquid micron-sized perfluorocarbon (PFC) droplets are currently being studied for use as ultrasound contrast agents [1], and cancer therapy via targeted drug delivery [2] or vessel occlusion [3]. Injected intravenously, PFC droplets are small enough to circulate within the bloodstream. Composed of a liquid PFC core and stabilized by lipids, polymers, surfactants, or albumin, droplets have a longer circulation half-life than microbubbles. However they have poor ultrasound contrast due to a similar acoustic impedance to that of the blood. Vaporization of the perfluorocarbon liquid to a gas bubble has been demonstrated using a technique called acoustic droplet vaporization [4], in which ultrasound irradiation of sufficient pressure amplitude induces the phase change from liquid to gas. Once vaporized into a gas bubble, the ultrasound contrast increases dramatically.

This research proposes an alternative method of droplet vaporization using a method we term optical droplet vaporization (ODV). By incorporating optical absorbing nanoparticles into the liquid core, vaporization could be induced via laser irradiation instead of ultrasound. The droplets could be used as photoacoustic contrast agents by measuring the photoacoustic signal using a low laser fluence (or a wavelength that is not close to the peak optical absorption of the nanoparticles) without inducing vaporization. Good contrast could be achieved in comparison to the surrounding tissue, which would potentially have negligible optical absorption. The droplets could also be used for cancer therapy in a similar method as proposed with acoustic droplet vaporization, either by the delivery of a drug enclosed in the droplet or by occluding blood vessels that supply the tumor [2,3].

This work investigates the potential of using PFC droplets as a dual contrast agent for ultrasound and photoacoustic imaging by examining their acoustic and photoacoustic properties. Ultra-high frequency (over 100 MHz) acoustic microscopy is capable of a resolution up to 1 μm at 1 GHz, and can be used to determine individual droplet size and sound velocity as they undergo vaporization [5], [6]. Droplets deposited onto a substrate can be analyzed using the time of flight of the ultrasound echoes from the droplet surface (t_1), the droplet-substrate interface (t_2) and the substrate beside the droplet (t_0). From these measurements, the droplet diameter d can be found using

Photons Plus Ultrasound: Imaging and Sensing 2011, edited by Alexander A. Oraevsky, Lihong V. Wang,
Proc. of SPIE Vol. 7899, 78993H · © 2011 SPIE · CCC code: 1605-7422/11/$18 · doi: 10.1117/12.875401

$$d = \frac{c_0}{2}(t_0 - t_1), \tag{1}$$

and the droplet sound velocity c_d found using

$$c_d = \frac{c_0}{2}\frac{(t_0 - t_1)}{(t_2 - t_1)}, \tag{2}$$

where c_0 is the sound velocity in the coupling fluid.

Photoacoustic measurements can be used to characterize droplets by measuring the photoacoustic signal produced during laser irradiation (and prior to any droplet conversion). Absorption of the light by the nanoparticles within the spherical droplets will cause the droplet to undergo a rapid thermoelastic expansion. Assuming that the droplet can be approximated as a sphere with homogeneous optical absorption, this expansion creates a pressure wave measured at a distance r from the droplet

$$p(q) = i\mu_a I_0 A e^{-iq\tau}\frac{(\sin q - q\cos q)/q^2}{(1-\rho)(\sin q/q) - \cos q + ic\rho\sin q}, \tag{3}$$

$$\text{with } A = \frac{dc_d\beta}{4\pi C_p(r/a)}, \tag{4}$$

where β is the thermal expansion coefficient, C_p is the heat capacity, μ_a is the absorption coefficient of the droplet (nanoparticles), ρ and c are the ratios of the density and sound velocity between the droplet and coupling fluid, respectively, and the time τ and frequency q are redefined as dimensionless quantities where $q = 2\pi fa/c_d$ and $\tau = (v/a)[t-(r-a)/c_0]$ is the delay time from the radius of the droplet [7].

2. METHOD

2.1 PFC Emulsions

PbS nanoparticles were synthesized [8], coated with silica [9, 10], and solubilized into PFC [11]. PFC droplets containing nanoparticles were prepared using deionized water, nanoparticle-PFC solution, and an anionic phosphate fluorosurfactant. Micron-scale droplets were prepared by coarse emulsification by vortexing followed by membrane emulsification using polymer membranes.

2.2 Photoacoustic Microscope

A commercially available SASAM acoustic microscope (Kibero GmbH, Germany) was modified to enable photoacoustic measurements. The acoustic microscope consists of an Olympus IX81 inverted optical microscope (Olympus, Japan) with an acoustic module positioned above the optical objective, which allows for precise sample targeting and simultaneous optical and acoustic/photoacoustic measurements [6], [12]. A 1064 nm laser (Teem Photonics, France) was collimated through the back port of the microscope and focused by a 10x optical objective (0.3 numerical aperture) onto the sample, focusing the laser to a approximately a 4 μm spot size.

The laser had a pulse width of 700 ps with a repetition frequency of up to 2 kHz, and the laser fluence could be adjusted up to 3.8 J/cm^2 per pulse. A 375 MHz transducer with a 60° aperture angle and -6 dB bandwidth of 42% was used for all measurements. Signals were amplified by a 40 dB amplifier then digitized at a rate of 8 GHz. In photoacoustic mode, signals were digitized at a rate of 2 kHz which was limited by the laser repetition frequency. In acoustic mode, a monocycle pulse generator generated 10 V_{pp} pulses with a center frequency of 300 MHz with 100% bandwidth at a pulse repetition frequency of 500 kHz. Details can be found in other publications [6],[12].

2.3 Acoustic and Photoacoustic Measurements

Acoustic and photoacoustic measurements were made on droplets deposited onto a 50 μm thick agar phantom. An agar phantom was used to reduce the ultrasound echo amplitude from the substrate under the droplet, which is typically a glass substrate and produces very strong ultrasound echoes. The phantom was made as thin as possible to minimize any light scattering during laser irradiation.

Pulse echo measurements were made directly over droplets to determine the diameter and sound velocity within the droplet. The time of flight echoes from the agar phantom surface (t_0), droplet surface (t_1) and droplet-phantom interface (t_2) were used in equations 1 and 2 to determine the diameter and sound velocity of nine droplets with diameters ranging from 3.2 to 6.7 μm. Pulse echo measurements were also made on droplets deposited onto a glass substrate to determine how the ultrasound backscatter amplitude, acoustic impedance and attenuation changed before and after optical droplet vaporization.

Photoacoustic measurements were made on three droplets of varying diameters, all less than 10 μm. These droplets were different than those measured acoustically. The diameter could not be accurately determined using optical methods due to poor contrast through the agar phantom. The photoacoustic signal was measured over a 15x15 μm area using a step size of 0.5 μm and 100 point averaging. A bandpass filter (110-800 MHz) was applied to reduce noise. The Fourier transform of four a-scans around the center of the droplet were averaged to determine the spectrum, then the reference spectrum (response of the transducer) was subtracted, as done in acoustic measurements [13]. The reference spectrum was obtained by measuring the photoacoustic signal from a black ink spot drawn on a glass slide. The resulting spectra were compared to theory predicted using equation 3.

3. RESULTS AND DISCUSSION

3.1 Pulse Echo Measurements

Acoustic measurements were used to determine the ultrasound backscatter from droplets deposited onto an agar phantom. Pulse echo measurements on the droplet and the agar phantom beside the droplet were completed using the 375 MHz transducer. Typical signals measured from the phantom surface and droplet are shown in figure 1. The time of flight of the echoes from the substrate (t_0), droplet surface (t_1) and droplet-phantom interface (t_2) were used in equations 1 and 2 to determine the diameter and sound velocity of nine droplets as shown in table 1. A coupling fluid sound velocity of 1521 m/s, the sound velocity of water at 36°C was used in this calculation. The diameter of the droplets ranged from 3.2 to 6.7 μm, and the sound velocity ranged from 311 to 406 m/s. Assuming an uncertainty of 0.25 ns in finding the central peak of the backscattered signal, the resulting errors in the sound velocity calculation are shown in table 1. The average sound velocity over the nine droplets was 351 ± 35 m/s. The beamwidth of the 375 MHz transducer was 4.0 μm, therefore for small droplets the acoustic plane wave at the transducer focus would cover the entire droplet, and therefore would correspond to scattering from a sphere rather than a planar surface. Higher sound velocities were measured for droplets with diameters greater than 4.0 μm, and if droplets with diameters 4.0 μm or less were excluded the average sound velocity over five droplets was 379 ± 18 m/s.

Table 1. The diameter and sound velocity of nine droplets determined using pulse echo methods and a 375 MHz transducer. The errors are calculated given an uncertainty of 0.25 ns in the accuracy of determining the peak from each ultrasound echo. The average sound velocity was 351 ± 35 m/s over all droplets, and 379 ± 18 m/s for droplets larger than 4.0 μm.

Droplet Number	Diameter (μm)	Sound Velocity (m/s)
1	3.2 ± 0.3	313 ± 23
2	3.3 ± 0.3	313 ± 22
3	3.6 ± 0.3	311 ± 20
4	4.0 ± 0.3	333 ± 20
5	4.6 ± 0.3	380 ± 20
6	5.5 ± 0.3	383 ± 17
7	5.9 ± 0.3	366 ± 15
8	6.5 ± 0.3	406 ± 16
9	6.7 ± 0.3	358 ± 13

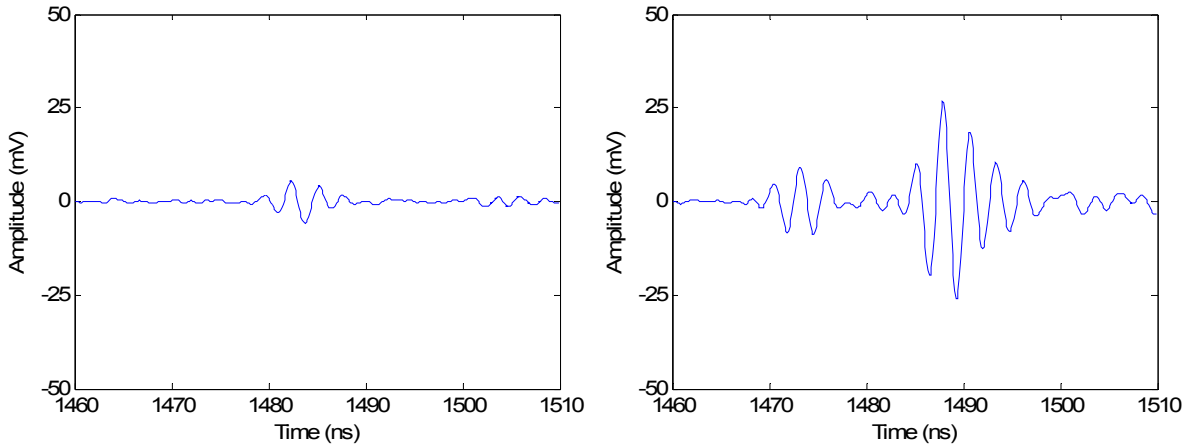

Figure 1: An ultrasound RF-line from the phantom surface measured beside the droplet (left) and directly over a droplet (right) measured using a 375 MHz transducer.

3.2 Photoacoustic Measurements

The photoacoustic signal was measured for droplets of three different diameters, all less than 10 μm using a laser fluence of 1.0 J/cm^2 and a 375 MHz transducer. The time domain signal and frequency spectra are shown in figure 2. The spectra were normalized to account for the transducer response by subtracting the reference signal (photoacoustic signal measured from a black ink spot) from the signal measured from the droplet in the frequency domain, as done in acoustic measurements [13].

The photoacoustic pressure amplitude as a function of frequency was calculated using equation 3, a density of 1650 kg/m^3, and two different sound velocities; 379 m/s (obtained from section 3.1), and 484 m/s (estimated from literature). A sound velocity of 484 m/s was estimated from literature by using the experimentally determined sound velocity of 527 m/s in [14] at 20°C, and linearly extrapolating to 36°C using a slope of -2.67 m/s/°C from [15]. Two sound velocities were used in the model, as variations in the sound velocity have been reported in literature and there are no measurements at the ultrasonic frequencies used in this study. The diameter of the droplet could not be determined using an optical scale due to the difficulty in accurately determining droplet edges through the agar phantom. The diameter was adjusted in equation 3 until the spectral features of the model matched the measured data for each sound velocity. While the exact diameter was unknown, the estimated diameter from the model were within our expectations.

Figure 2 shows the measured photoacoustic signal compared to the model, where the constant A was set to unity, as this parameter only affects the signal amplitude. All spectra were normalized to the maximum amplitude. Good agreement in the location and number of spectral features was observed between theory and experiment for all three droplets of different sizes. The agreement was not as good past 500 MHz, which was outside of the -6 dB bandwidth of the transducer. A decrease in signal as a function of frequency agreed well with theory with the 3 μm droplet, however the agreement became worse with increasing droplet size. As the laser beam itself has a 4 micron spot size, it is not known if this was due to a non-uniform illumination pattern of the droplet or other reasons.

3.3 Droplet Vaporization

Vaporization of droplets was observed for laser fluence levels above approximately 1.5 J/cm^2. In the acoustic vaporization process studied by Kripfgans and colleagues, a rapid expansion of the droplet occurs, followed by a much slower expansion [4]. In these experiments, immediately after irradiation with a single laser pulse of sufficient intensity, a rapid increase in the droplet diameter (measured optically) was observed expanding to approximately 5-10x the original droplet size immediately after vaporization. The converted droplet then continued expanding at a rate of approximately 0.1-0.2 μm/s (measured optically over time). To confirm that vaporization occurred, pulse echo measurements were performed on the bubble 10 seconds following vaporization. Measurements immediately following vaporization was not possible due to a delay when switching the acoustic microscope from photoacoustic to acoustic mode. The laser irradiation occurs with the instrument in photoacoustic mode.

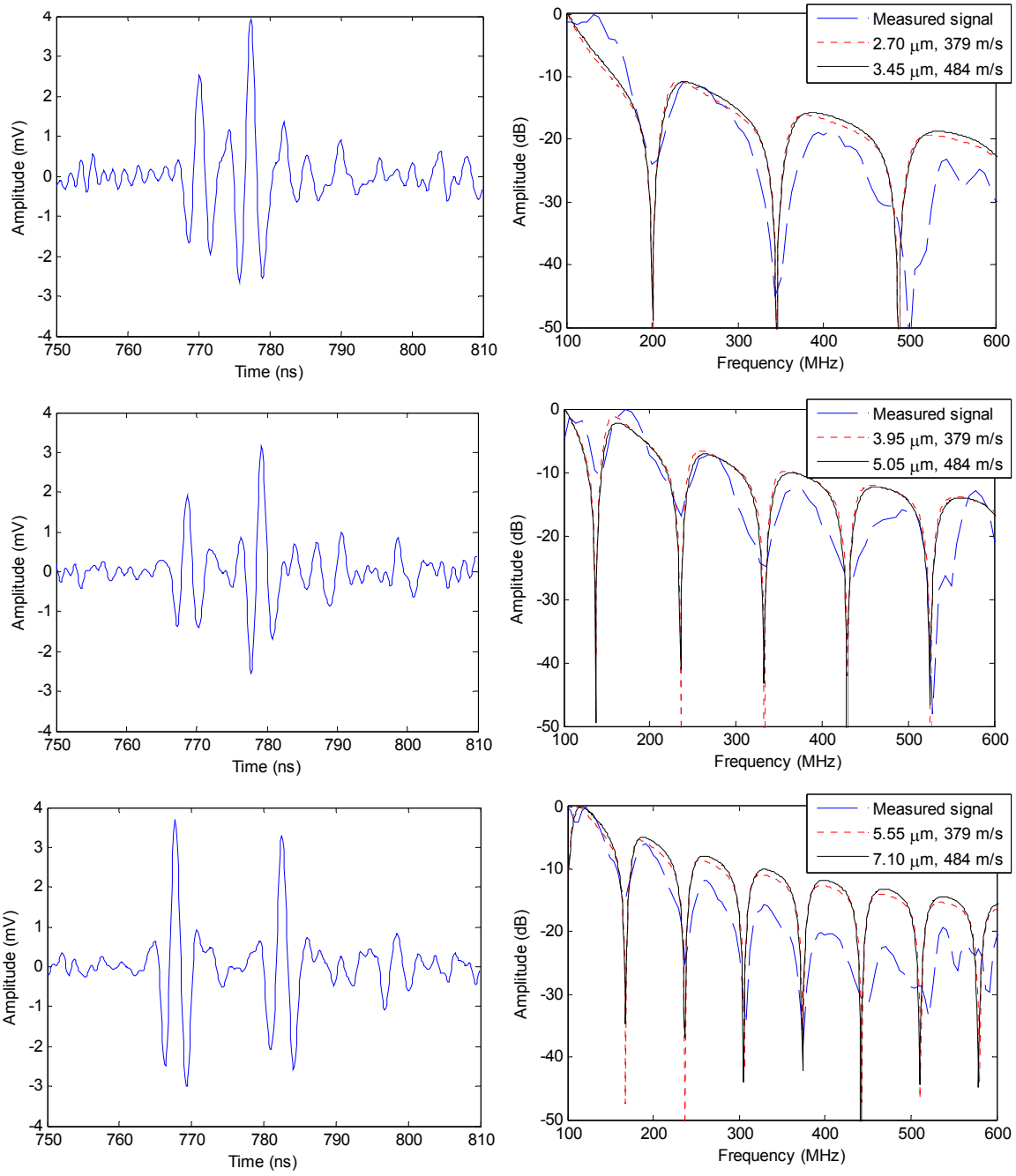

Figure 2: Time domain signal (left) and corresponding normalized frequency spectra (dashed line, right) of three PFC droplets. The theoretical model was calculated using equation 3 with a density of 1650 kg/m^3 and a sound velocity of 379 m/s (dotted line), and 484 m/s (solid line). The droplet diameter was adjusted to match the model spectrum features to the measured photoacoustic spectrum.

With the 375 MHz transducer focused directly on the droplet, the pulse echo measurements indicated an increase in the ultrasound backscatter amplitude from 40-60 mV (droplet) to 300-400 mV (bubble). The backscatter amplitude from the bubble was likely higher than what was recorded, as during the 10 second delay in switching to acoustic mode, the bubble grew in size and the bubble surface would have expanded past the focal region of the transducer, reducing the transducer geometric gain. Since the sensitivity of the transducer decreases away from the transducer focus, a direct

comparison of the backscatter amplitude before and after vaporization was not performed in this study as it would require a correction for spatial variations in the axial profile. The increase in backscatter amplitude indicated an increase in the reflection coefficient, and therefore acoustic impedance after vaporization to a bubble.

The existence of the threshold exposure value required for the conversion of the liquid droplet to a gas bubble confirms that these can be used as dual-mode contrast agents. The liquid droplets can be detected photoacoustically while simultaneously avoiding conversion if laser intensities are either low enough, or laser illumination wavelengths are used that are far from the nanoparticle optical absorption peaks. As one of the main target applications is molecular imaging, the presence of the droplets at the region of interest can be detected using photoacoustic imaging, and then the droplets can be converted to either occlude vessels in the region of interest, or to deliver the appropriate drug payload as proposed by Fabiilli et al. [2]. We have shown in other work [16] that droplets of 300 nm diameter could be reproducibly vaporized. The larger micron-sized droplet size (1-5 μm), would be restricted to the vasculature, whereas the nanometer-sized droplets can traverse through the tumor vasculature into the tumor interstisium and accumulate in tumors due to the enhanced permeability and retention effect [17]. The work presented in this paper further characterizes these droplets, both acoustically and photoacoustically, so that imaging and therapy protocols could be optimized.

4. CONCLUSIONS

An initial investigation of the acoustic and photoacoustic characterization of micron-sized liquid PFC droplets was presented. Acoustic measurements at 375 MHz were used to determine the diameter and sound velocity of nine droplets, which ranged from 3.2 to 6.7 μm, and 311 to 406 m/s, respectively. Droplet vaporization was observed above a laser fluence of 1.5 J/cm^2. Acoustic measurements also verified vaporization occurred, as indicated by the increase in the acoustic backscatter amplitude, acoustic impedance and attenuation through the droplet. Additionally, photoacoustic measurements on three droplets with different diameters showed good agreement to the theoretical photoacoustic pressure generated from a liquid sphere.

5. ACKNOWLEDGEMENTS

E. Strohm is supported through a NSERC doctoral scholarship. This research was undertaken, in part, thanks to funding from NSERC and the Canada Research Chairs Program awarded to M. Kolios. Funding to purchase the equipment was provided by the Canada Foundation for Innovation, the Ontario Ministry of Research and Innovation, and Ryerson University. This study was supported, in part, by the CIHR Excellence in Radiation Research for the 21st century (EIRR21) Research Training Program, the Ontario Institute for Cancer Research Network through funding provided by the Province of Ontario, the FY07 Department of Defense Breast Cancer Research Program Concept Award (BC075873) and a program project grant entitled “Imaging for Cancer” from the Terry Fox Foundation.

REFERENCES

[1] Wilson, K., Homan, K., and Emelianov, S., “Photoacoustic and ultrasound imaging contrast enhancement using a dual contrast agent,” Proc. SPIE 7564, 75642P-75642P-5 (2010).

[2] Fabiilli, M.L., Haworth, K.J., Sebastian, I.E., Kripfgans, O.D., Carson, P.L., Fowlkes, J.B., “Delivery of chlorambucil using an acoustically-triggered perfluoropentane emulsion,” Ultrasound in Medicine and Biology 36(8), 1364-75 (2010).

[3] Kripfgans, O.D., Fowlkes, J.B., Woydt, M., Eldevik, O.P., Carson, P.L., “In vivo droplet vaporization for occlusion therapy and phase aberration correction,” IEEE Transactions on Ultrasonics, Ferroelectrics, and Frequency Control 49(6), 726-738 (2002).

[4] Kripfgans, O., Fowlkes, J., Miller, D., Eldevik, O., and Carson, P., “Acoustic droplet vaporization for therapeutic and diagnostic applications,” Ultrasound in Medicine and Biology 26(7), 1177-1189 (2000).

[5] Briggs, G.A.D., Wang, J., Gundle, R., “Quantitative acoustic microscopy of individual living human cells,” Journal of Microscopy 172(1), 3-12 (1993).

[6] Strohm, E.M., Czarnota, G.J., Kolios, M.C., “Quantitative Measurements of Apoptotic Cell Properties Using Acoustic Microscopy,” IEEE Transactions on Ultrasonics, Ferroelectrics, and Frequency Control 57(10), 2293-2304 (2010).

[7] Diebold, G.J., Sun, T., Khan, M.I., “Photoacoustic monopole radiation in one, two, and three dimensions,” Physical Review Letters 67(24), 3384-3387 (1991).
[8] Hines, M.A., Scholes, G.D., “Colloidal PbS nanocrystals with size-tunable near-infrared emission: Observation of post-synthesis self-narrowing of the particle size distribution,” Advanced Materials 15(21), 1844-1849 (2003).
[9] Gorelikov, I., Matsuura, N., “Single-step coating of mesoporous silica on cetyltrimethyl ammonium bromide-capped nanoparticles”, Nano Lett. 8(1), 369-373 (2008).
[10] Yi, D.K., Selvan, S.T., Lee, S.S., Papaefthymiou, G.C., Kundaliya, D., Ying, J.Y., "Silica-coated nanocomposites of magnetic nanoparticles and quantum dots,” J. Am. Chem. Soc. 127(14), 4990-4991 (2005).
[11] Matsuura, N., Gorelikov, I., Williams, R., Wan, K., Zhu, S., Booth, J., Burns, P., Hynynen, K., Rowlands, J.A. “Nanoparticle-Tagged Perfluorocarbon Droplets for Medical Imaging,” Materials Research Society Symposium Proceedings 1140, 87-92 (2009).
[12] Rui, M., Narashimhan, S., Bost, W., Stracke, F., Weiss, E., Lemor, R., Kolios, M.C., “Gigahertz optoacoustic imaging for cellular imaging,” Proc. SPIE 7564, 756411-756411-6 (2010).
[13] Baddour, R.E., Sherar, M.D., Hunt, J.W., Czarnota, G.J., Kolios, M.C., “High-frequency ultrasound scattering from microspheres and single cells,” The Journal of the Acoustical Society of America 117(2), 934 (2005).
[14] Hasi, W.L., Lu, Z.W., Gong, S., Liu, S.J., Li,Q., and He, W.M., “Investigation of stimulated Brillouin scattering media perfluoro-compound and perfluoropolyether with a low absorption coefficient and high power-load ability,” Applied optics 47(7), 1010-4 (2008).
[15] Marsh, J.N., Hall, C.S., Wickline, S.A., Lanza, G.M., “Temperature dependence of acoustic impedance for specific fluorocarbon liquids,” J Acoust Soc Am. 12(6), 2858-62 (2002).
[16] Strohm, E., Rui, M., Gorelikov I., Matsuura, N., Kolios, M., “Optical Droplet Vaporization (ODV): photoacoustic characterization of perfluorocarbon droplets”, IEEE Ultrasonics Symposium 2010 (in print).
[17] Hobbs, S.K., Monsky, W.L., Yuan, F., Roberts, W.G., Griffith, L., Torchilin V.P., Jain, R.K., "Regulation of transport pathways in tumor vessels: role of tumor type and microenvironment," Proc Natl Acad Sci USA 95(8), 4607-12 (1998).